Supporting Information

Steiner *et al.* 10.1073/pnas.0804034105

SI Text

Results. ***The fluorophore-labeled D135–L14 ribozyme is catalytically competent.*** The activity of the *in vitro* transcribed (1) D135–L14 construct was measured in a single-turnover cleavage assay with the substrates 17/7 under optimal conditions for self-splicing (2) and compared with the unmodified D135 construct (Fig. S3*A*), clearly indicating that our labeling scheme only minimally affects the cleavage activity of the ribozyme. The unmodified ribozyme yields a cleavage rate constant $k_{obs} = 0.40 \pm 0.02$ min^{-1}, whereas the D135–L14 ribozyme, which includes the modular loops but not the fluorophore labels, resulted in k_{obs} values up to 0.37 ± 0.02 min^{-1}. In the presence of the fluorophore- and biotin-labeled DNA-oligonucleotides, the cleavage rate was only reduced by 27% ($k_{obs} = 0.27 \pm 0.01$ min^{-1}). The final fraction of product formation was 85% and remained comparable for all constructs. These results correspond well with earlier values for the unmodified D135 ribozyme (2), giving evidence that our D135–L14 ribozyme behaves accordingly.

Group II introns are known to require high ionic strength for optimal activity *in vitro* (3, 4), which is thought to be caused by high Mg^{2+} requirement for compaction of D1 and stabilization of the native state (5). We measured the Mg^{2+} requirement for the fluorophore- and biotin-labeled D135–L14 ribozyme using cleavage assays in the presence of Mg^{2+} ranging from 0 to 100 mM. The observed cleavage rate constants are shown as a function of Mg^{2+} concentration in Fig. S3*B*. This experimental data were fit to the Hill equation (**S2**) to yield the dissociation constant, $K_{Mg} = 52.7 \pm 3.4$ mM, which is comparable to reported values ($K_{Mg} = 20–40$ mM) (6, 7), illustrating that our fluorophore-labeled D135–L14 performs catalysis much like D135.

The fluorophore-labeled D135–L14 ribozyme requires Mg^{2+} ions for folding. We characterized the folding behavior of freely diffusing fluorophore-labeled D135–L14 in solution to determine the role of Mg^{2+} in folding independent of catalysis at 42°C. The fluorescence emission spectrum in absence of Mg^{2+} shows two bands for the donor and acceptor fluorophores, respectively (Fig. 2*A*). The donor intensity at 565 nm is higher than the acceptor at 665 nm, and the observed FRET ratio is 0.275. Upon addition of 100 mM Mg^{2+}, the donor intensity decreases slightly, whereas the acceptor increases. As a result, the overall FRET ratio increases exponentially to 0.290 with a rate constant $k_{obs} = 0.90 \pm 0.07$ min^{-1} (Fig. 2*B*), indicating the presence of a (sub)portion of compacted molecules in which the fluorophores draw nearer. This rate is in very good agreement with the $k_{obs} \approx 1$ min^{-1} for the rate-limiting step of D1 compaction obtained from hydroxyl radical footprinting, NAIM studies, and ribozyme activity assays (5, 7, 8).

The FRET increase to 0.295 in this bulk experiment suggests that a conformational change takes place in the presence of Mg^{2+} ions, during which the relative distance between the fluorophores on the RNA decreases. To determine the dissociation constant, the observed FRET ratio was plotted as a function of Mg^{2+} concentration (Fig. 2*C*) and fit with Eq. **S2**, yielding $K_{Mg} = 42.3 \pm 1.3$ mM. This value is again in very good agreement with the K_{Mg} from the cleavage reaction described above as well as reported values for D135 (6, 7).

Methods: Single-Turnover Cleavage Assay. The substrates 17/7 and 17/7-dC were 5′-labeled with [γ-^{32}P]ATP and T4 DNA ligase using standard procedures. DNA-oligonucleotides were in 6-fold excess over D135–L14 to avoid unbound ribozyme in the experiments. Cy3-DNA, Cy5-DNA, and T-biotin-DNA (600 nM) were heat-annealed to D135–L14 (100 nM) at 90°C for 1 min in reaction buffer [80 mM Mops (pH 6.9), 500 mM KCl] followed by Mg^{2+} addition and incubation at 42°C for 15 min in varying amounts of $MgCl_2$. ^{32}P-labeled 17/7 or 17/7-dC (1 nM) was separately incubated in reaction buffer and $MgCl_2$ and then added to annealed, biotinylated, and Cy3/Cy5-labeled ribozyme to start the cleavage reaction. Cleavage reactions were carried out at 42°C as well as at room temperature. Aliquots (1 μl) were removed from the reaction mixture (20 μl) at specific points in time and analyzed on 18% polyacrylamide gels. Reaction rate constants were determined by quantification of the gels and fitting to single-exponential expression:

$$\text{frac[product]} = (1 - A_1) - A_2 \times e^{-kt} \qquad \textbf{[S1]}$$

with A_1 being the fraction of uncleaved substrate, A_2 the fraction of product formed, and k the first-order rate constant in minutes^{-1}.

The first-order rate constants were plotted with respect to increasing [Mg^{2+}] and fit to a modified Hill equation

$$y = y_0 + \frac{x^n}{K_{Mg}{}^n + x^n} \qquad \textbf{[S2]}$$

where K_{Mg} is the [Mg^{2+}] at half-maximum rate and n represents the cooperativity constant.

1. Gallo S, Furler M, Sigel RKO (2005) *In vitro* transcription and purification of RNAs of different size. *Chimia* 59:812–816.
2. Su LJ, Brenowitz M, Pyle AM (2003) An alternative route for the folding of large RNAs: Apparent two-state folding by a group II intron ribozyme. *J Mol Biol* 334:639–652.
3. Sigel RKO (2005) Group II intron ribozymes and metal ions: A delicate relationship. *Eur Inorg Chem* 12:2281–2292.
4. Lehmann K, Schmidt U (2003) Group II introns: Structure and catalytic versatility of large natural ribozymes. *Crit Rev Biochem Mol Biol* 38:249–303.
5. Su LJ, Waldsich C, Pyle AM (2005) An obligate intermediate along the slow folding pathway of a group II intron ribozyme. *Nucleic Acids Res* 33:6674–6687.
6. Fedorova O, Zingler N (2007) Group II introns: Structure, folding and splicing mechanism. *Biol Chem* 388:665–678.
7. Swisher JF, Su LJ, Brenowitz M, Anderson VE, Pyle AM (2002) Productive folding to the native state by a group II intron ribozyme. *J Mol Biol* 315:297–310.
8. Pyle AM, Fedorova O, Waldsich C (2007) Folding of group II introns: A model system for large, multidomain RNAs? *Trends Biochem Sci* 32:138–145.
9. Rangan P, Masquida B, Westhof E, Woodson SA (2003) Assembly of core helices and rapid tertiary folding of a small bacterial group I ribozyme. *Proc Natl Acad Sci USA* 100:1574–1579.

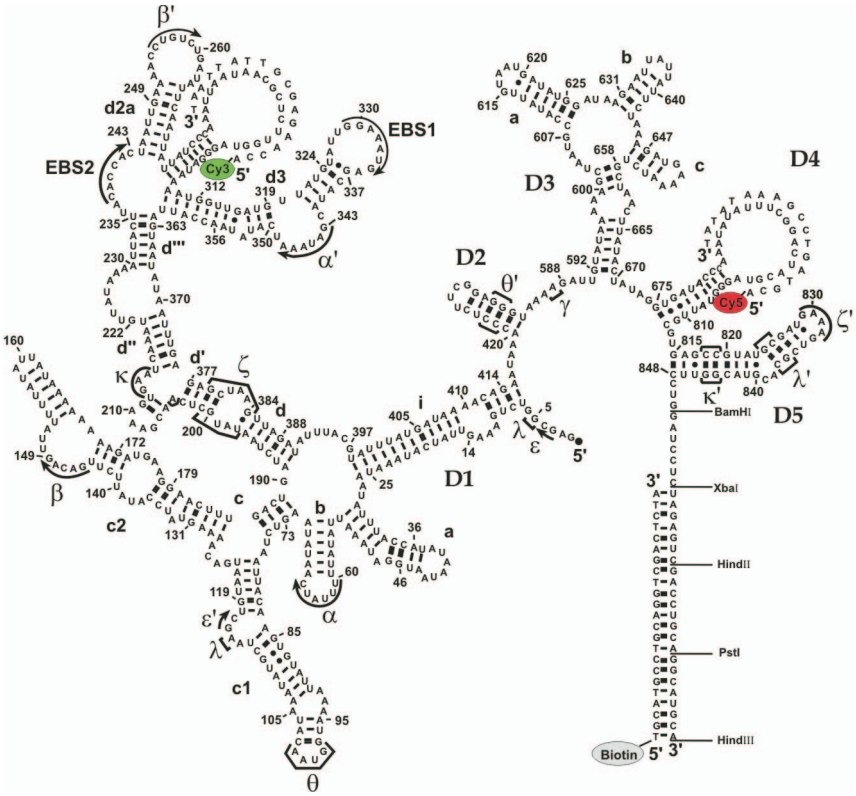

Fig. S1. Primary and secondary structure of the D135–L14 ribozyme derived from the ai5γ group II intron from the *cox 1* gene in *S. cerevisiae*. The two modular loops, which bind two oligonucleotides with the fluorophores Cy3 (green marker) or Cy5 (red marker) at their 5′ end, are inserted in the d2b hairpin in D1 and into D4 as indicated. The numbering corresponds to the WT sequence, and the tertiary interactions are indicated by Greek letters. The 3′ end of the intron is elongated to bind to a 5′-biotinylated complementary DNA-oligonucleotide for attachment on the quartz surface carrying the counterpart streptavidin. Cy3 label is depicted in green, Cy5 label in red and biotin in gray.

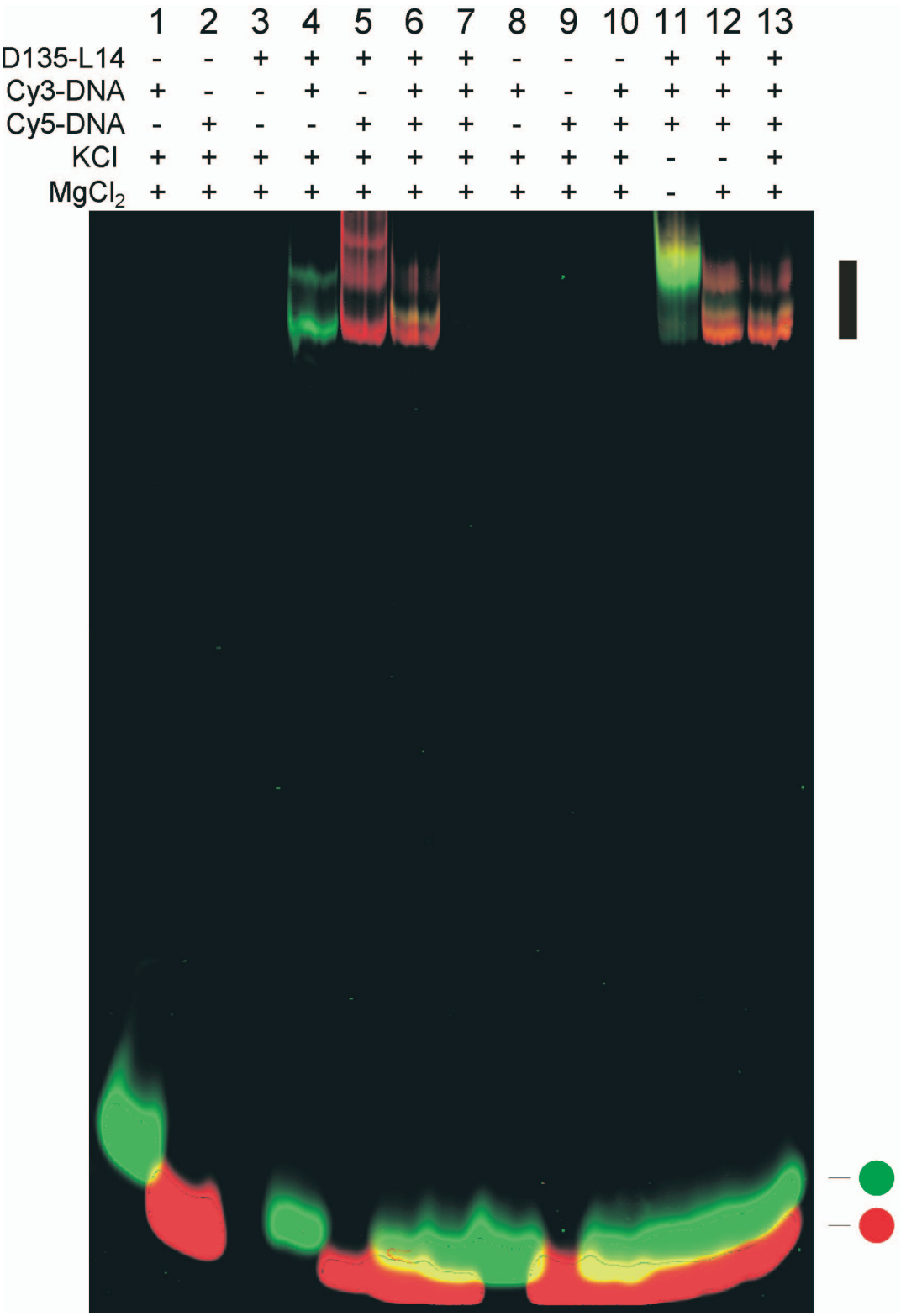

Fig. S2. Hybridization of Cy3-DNA and Cy5-DNA to D135–L14 detected on nondenaturing gel by fluorescence. The RNA–DNA hybrids (indicated by black bar on right) are shifted relative to the free DNA-oligonucleotides (Cy3-DNA, green circle; Cy5-DNA, red circle). Amount of Cy3-DNA is kept at 10 nmol and Cy5-DNA is constant at 10 nmol except for lanes 6 and 10, where it is doubled to 20 nmol. D135–L14 is present at 15 nmol, except for lane 7, where it is reduced to 1.8 nmol to simulate ratios used in bulk FRET experiments. KCl concentration is at 0.5 M, apart from lane 13, where it is reduced to 0.1 M. $MgCl_2$ concentration is constantly 6 mM. Samples were prepared analogously to FRET measurements before native gel (6% wt/vol) electrophoresis run at 4°C [3 mM MgOAc and 66 mM Hepes, 34 mM Tris (pH 7.4) (room temperature)] (9).

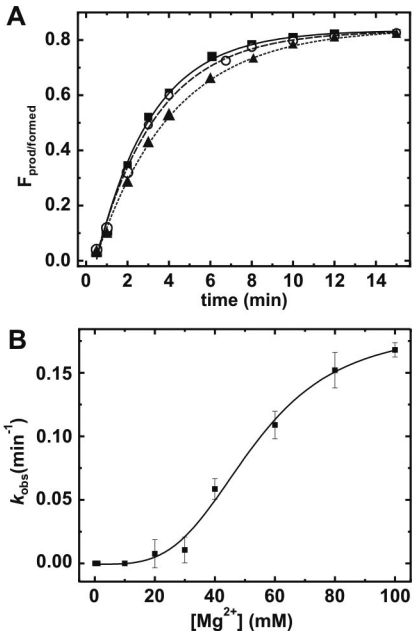

Fig. S3. Splicing activity of the D135–L14 ribozyme. (*A*) Product formation in single-turnover cleavage assays with 5′-labeled 17/7 substrate together with the experimental fit for D135 (■, solid line), D135–L14 (○, dashed line) as well as FRET-labeled and biotinylated D135–L14 (▲, dotted line). Rate constants k_{obs} are 0.40 ± 0.02, 0.37 ± 0.02, and 0.27 ± 0.01 min^{-1}, respectively. (*B*) Mg^{2+} dependence of substrate cleavage by fully labeled D135–L14 and fit with Hill equation (**S2**) giving K_{Mg} = 52.7 ± 3.4 mM and $k_{obs,max}$ = 0.18 ± 0.01 min^{-1}. Error bars stem from two independent assays.

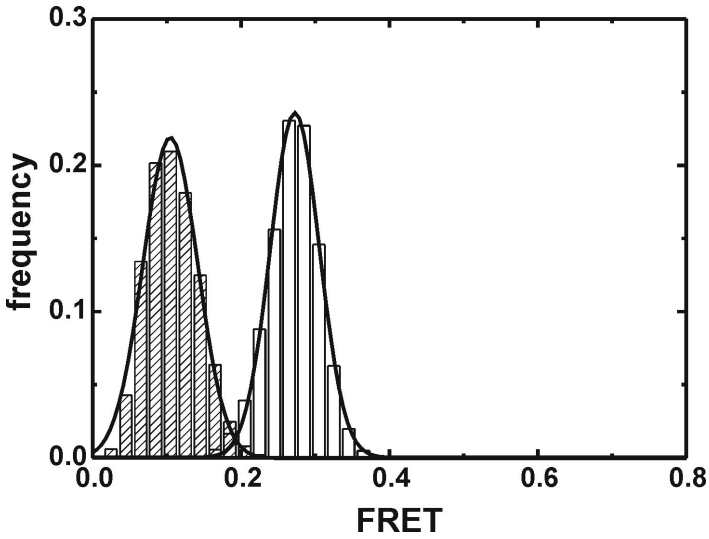

Fig. S4. FRET value of D135–L14 molecules in the U and I states. Molecules at conditions of 0 mM $MgCl_2$, 10 μM EDTA (dashed bars) show a FRET distribution at a mean peak value of $\approx$0.1 (U state). The FRET histogram at 1 mM $MgCl_2$ (white bars, see also Fig. 4) is shown for comparison (I state). The experiments were performed in 80 mM Mops (pH 7.0), 500 mM KCl.

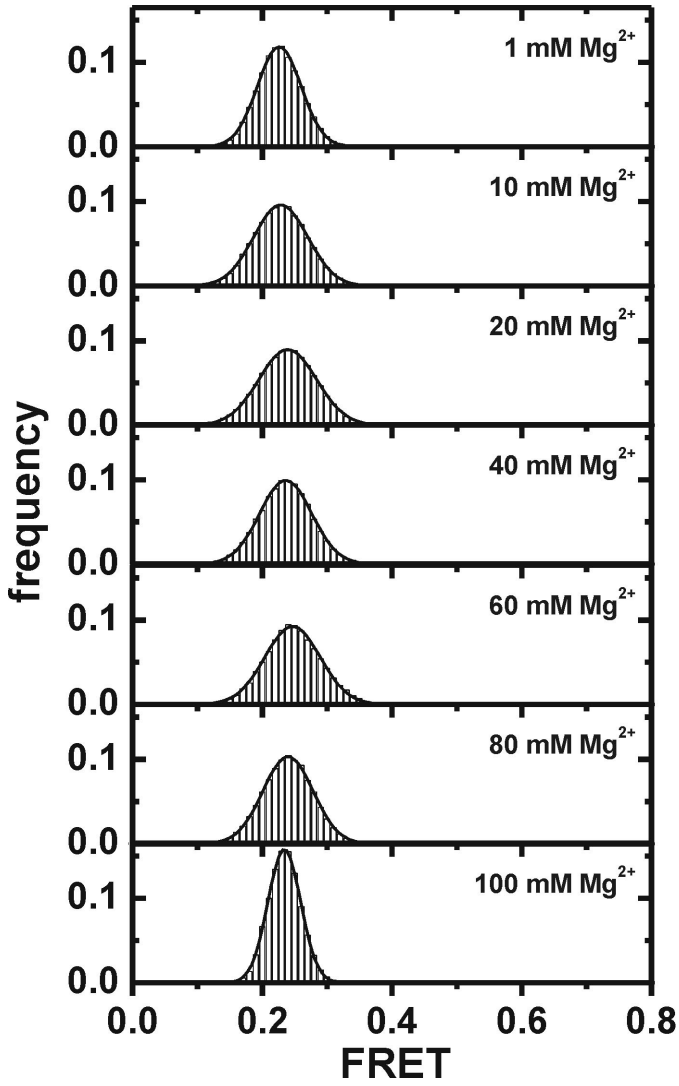

Fig. S5. FRET distribution of static D135–L14 molecules. All static molecules at 1, 10, 20, 40, 60, 80, and 100 mM show a FRET value ≈0.25.

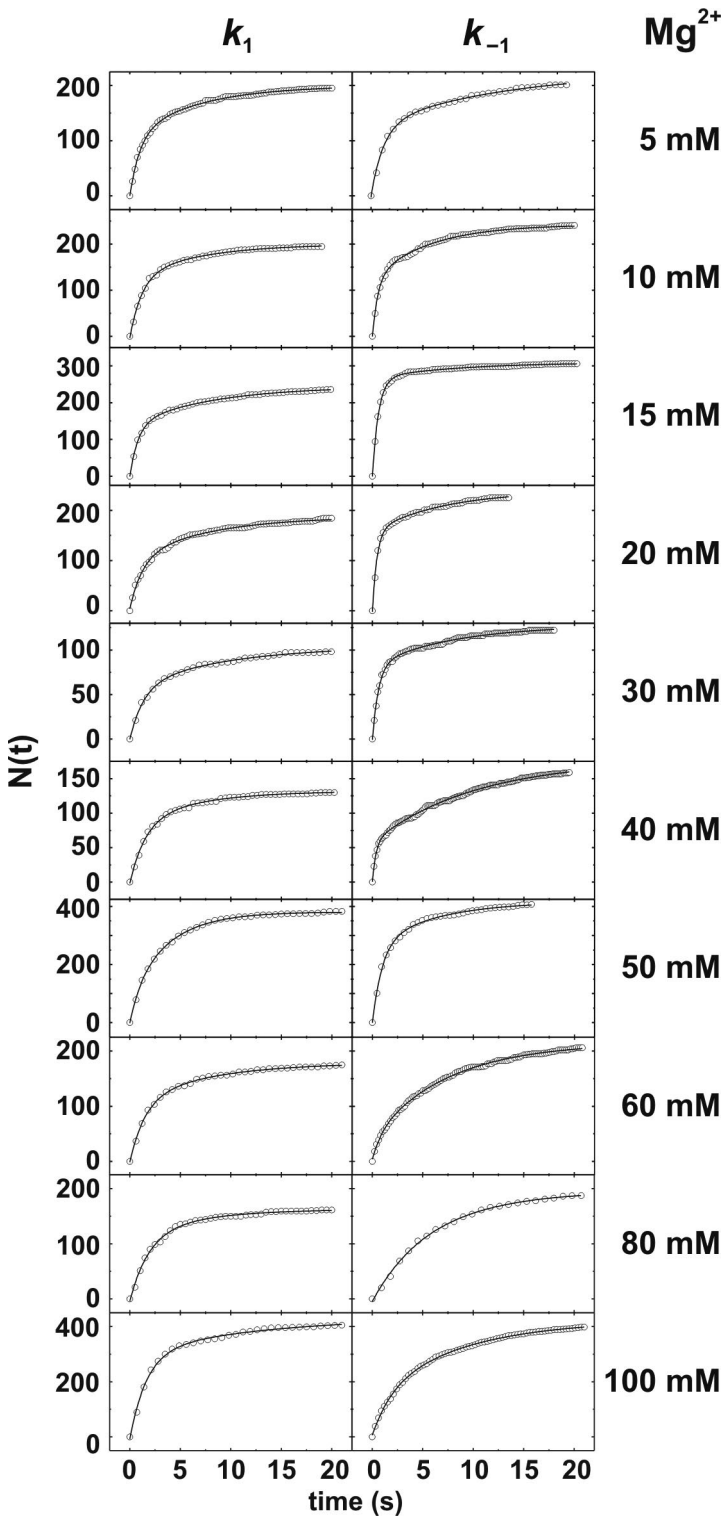

Fig. S6. Calculation of rates k_1 (*Left*) and k_{-1} (*Right*). The number of dwell times shorter than time *t* obtained from the integration of dwell time histograms at $MgCl_2$ concentration as indicated to the right together with double-exponential fits (black lines) is shown.

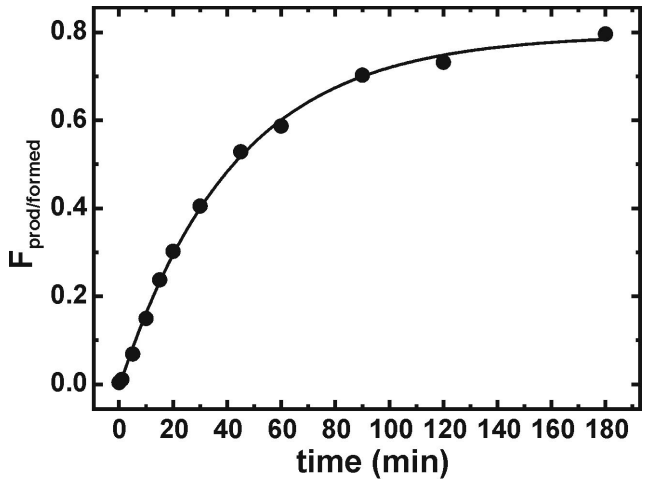

Fig. S7. D135–L14 cleavage activity at room temperature after incubation at 42°C. The cleavage rate obtained is $k_{obs} = 0.024 \pm 0.001$ min^{-1}.

Table S1. Rates k_1 and amplitudes A_1 from double-exponential fit at tested Mg^{2+} concentrations

$[Mg^{2+}]$, mM	$k_1(1)$	$A_1(1)$	$k_1(2)$	$A_1(2)$
5	1.00 ± 0.04	125 ± 7	0.13 ± 0.01	94 ± 1
10	0.84 ± 0.06	148 ± 13	0.13 ± 0.02	76 ± 2
15	1.22 ± 0.04	170 ± 9	0.11 ± 0.01	106 ± 1
20	0.80 ± 0.06	111 ± 11	0.11 ± 0.02	878 ± 2
30	0.73 ± 0.07	64 ± 7	0.09 ± 0.02	48 ± 1
40	0.65 ± 0.06	95 ± 11	0.14 ± 0.03	49 ± 3
50	0.95 ± 0.15	115 ± 31	0.24 ± 0.01	285 ± 8
60	0.65 ± 0.05	120 ± 11	0.11 ± 0.02	72 ± 2
80	0.55 ± 0.05	108 ± 8	0.18 ± 0.01	65 ± 1
100	0.66 ± 0.06	434 ± 34	0.06 ± 0.04	256 ± 11

Values are corrected as described in *SI Methods* ref. 10. The error limits correspond to 1 SD.

Table S2. Rates k_{-1} and amplitudes and A_{-1} from double-exponential fit at tested Mg^{2+} concentrations

$[Mg^{2+}]$, mM	$k_{-1}(1)$	$A_{-1}(1)$	$k_{-1}(2)$	$A_{-1}(2)$
5	1.52 ± 0.09	131 ± 19	0.13 ± 0.03	100 ± 3
10	1.87 ± 0.09	128 ± 16	0.16 ± 0.01	120 ± 1
15	1.64 ± 0.02	274 ± 10	0.10 ± 0.01	43 ± 1
20	2.24 ± 0.08	166 ± 18	0.12 ± 0.01	82 ± 1
30	1.66 ± 0.05	85 ± 6	0.11 ± 0.01	46 ± 1
40	2.87 ± 0.14	60 ± 12	0.08 ± 0.01	120 ± 1
50	1.02 ± 0.08	269 ± 38	0.14 ± 0.03	154 ± 6
60	0.49 ± 0.04	69 ± 5	0.07 ± 0.01	151 ± 1
80	0.17 ± 0.03	145 ± 12	0.08 ± 0.01	58 ± 4
100	0.51 ± 0.05	148 ± 14	0.09 ± 0.01	272 ± 4

Values are corrected as described in *SI Methods* ref. 10. The error limits correspond to 1 SD.